

# Stable Triple-Helical DNA Complexes Formed by Benzopyridoindole– and Benzopyridoquinoxaline– Oligonucleotide Conjugates

Gail C. Silver, Jian-Sheng Sun, Chi Hung Nguyen,<sup>†</sup> Alexandre S. Bourtine, Emile Bisagni,<sup>†</sup> and Claude Hélène\*

Contribution from the Laboratoire de Biophysique, Muséum National d'Histoire Naturelle, INSERM U201, CNRS URA 481, 43 rue Cuvier, 75231 Paris Cedex 05, France

Received April 22, 1996<sup>⊗</sup>

**Abstract:** Benzopyridoindole and benzopyridoquinoxaline derivatives were conjugated to a 14-mer oligonucleotide at either of two different positions: the 5' end or an internucleotide position in the center of the 14-mer. These oligonucleotide–intercalator conjugates were then tested for their ability to form stable DNA triple helices with a DNA target duplex under physiological conditions. All of the derivatives synthesized were found to do so. Two derivatives in particular, a benzo[*h*]pyridoquinoxaline (B[*h*]PQ) attached to the 5' end and a benzo[*e*]pyridoindole (B[*e*]PI) attached to the internal position on the phosphate diester backbone, dramatically stabilized the triple helix under physiological conditions. In the absence of spermine, the melting temperature of the triplex-to-duplex transition increased from 11 °C for a non-modified triplex to 38 and 37 °C, respectively, for the B[*h*]PQ and B[*e*]PI conjugates. Acridine-oligonucleotide conjugates were much less stable, melting at 25 °C (5' attachment) and at 23 °C (internucleotide linkage). In the presence of spermine, the melting temperature increased from 28 °C for a non-modified triplex to 51 and 54 °C for the B[*h*]PQ and B[*e*]PI conjugates, respectively, equivalent to a stabilization of ~4 kcal·mol<sup>-1</sup> at 37 °C. Furthermore, the conjugation of these intercalators to the third strand was not detrimental to the selectivity of recognition of the target duplex sequence. Molecular modeling reinforced and provided possible models for some of the intercalator–triple helix interactions investigated. These results demonstrate the possibility for forming stable DNA triple helices at physiological pH and temperature.

## Introduction

The regulation of gene expression by nucleic acids is a strategy that has the potential to be used for the treatment of genetic-based diseases.<sup>1–4</sup> Oligonucleotides may halt translation by specifically recognizing and binding to messenger RNA (antisense approach).<sup>5,6</sup> They may also impede transcription by binding to the major groove of double-stranded DNA (antigene approach).<sup>7,8</sup> In the latter approach, a (T,C)-containing third strand (pyrimidine motif) runs parallel to the duplex oligopurine strand and is bound through Hoogsteen hydrogen bonds, with the formation of T·A·T and C·G·C<sup>+</sup> triplets.<sup>9,10</sup> Alternatively, a (G,A)- containing third strand can bind in an antiparallel orientation with respect to the oligopurine target strand through reverse Hoogsteen hydrogen bonds, leading to the formation of C·G·G and T·A·A base triplets.<sup>11,12</sup> (G,T)-

containing oligonucleotides bind in either a parallel or an antiparallel orientation depending on the base sequence (i.e., length of G and T tracts and number of GpT/TpG steps).<sup>13</sup>

At present, there are several limitations to the development of the antigene strategy. Except for a few cases,<sup>14</sup> the stability of triple-helical complexes is usually weaker than that of double-helical complexes. In addition, the requirement for cytosine protonation in the pyrimidine motif limits triplex stability at neutral pH. One strategy to improve triplex stability is to covalently attach DNA intercalators to the third strand.<sup>7,15–17</sup> Acridine is an intercalator which is commonly used for this purpose due to its recognized ability to significantly stabilize triple helices when covalently attached to the probe strand.<sup>16–18</sup>

Benzopyridoindoles (BPI)<sup>19</sup> and benzopyridoquinoxalines (BPQ)<sup>20</sup> are classes of tetracyclic aromatic compounds (Figure 1) having antineoplastic activity. They have been shown to

<sup>†</sup> Laboratoire de Synthèse Organique, Institut Curie-Biologie, CNRS URA 1387, Bâtiment 110, 91405 Orsay, France

<sup>⊗</sup> Abstract published in *Advance ACS Abstracts*, December 1, 1996.

(1) Croke, S. T.; Lebleu, B. *Antisense Research and Applications*; CRC Press, Inc.: London, 1993.

(2) Hélène, C.; Toulmé, J.-J. *Biochim. Biophys. Acta* **1990**, *1049*, 99–125.

(3) Murray, J. A. H.; Crockett, N. In *Antisense RNA and DNA*; J. A. H. Murray, Ed.; John Wiley & Sons, Inc.: New York, 1992; Vol. 11; pp 1–48.

(4) Uhlmann, E.; Peyman, A. *Chem. Rev.* **1990**, *90*, 543–584.

(5) Pierga, J. Y.; Magdelenat, H. *Cell. Mol. Biol.* **1994**, *40*, 237–61.

(6) Stein, C. A.; Cheng, Y. C. *Science* **1993**, *261*, 1004–1012.

(7) Thuong, N. T.; Hélène, C. *Angew. Chem., Int. Ed. Engl.* **1993**, *32*, 666–690.

(8) Radhakrishnan, I.; Patel, D. J. *Biochemistry* **1994**, *33*, 11405–11416.

(9) Le Doan, T.; Perrouault, L.; Praseuth, D.; Habhoub, N.; Decout, J. L.; Thuong, N. T.; Lhomme, J.; Hélène, C. *Nucleic Acids Res.* **1987**, *15*, 7749–60.

(10) Moser, H. E.; Dervan, P. B. *Science* **1987**, *238*, 645–650.

(11) Beal, P. A.; Dervan, P. B. *Science* **1991**, *251*, 1360–1363.

(12) Pilch, D. S.; Levenson, C.; Shafer, R. H. *Biochemistry* **1991**, *30*, 6081–8.

(13) de Bizemont, T.; Duval-Valentin, G.; Sun, J.-S.; Bisagni, E.; Garestier, T.; Hélène, C. *Nucleic Acids Res.* **1996**, *24*, 1136–1143.

(14) Svinarchuk, F.; Paoletti, J.; Malvy, C. *J. Biol. Chem.* **1995**, *270*, 14068–14071.

(15) Hélène, C. *Br. J. Cancer* **1989**, *60*, 157–160.

(16) Sun, J. S.; François, J. C.; Montenay-Garestier, T.; Saison-Behmoaras, T.; Roig, V.; Chassignol, M.; Thuong, N. T.; Hélène, C. *Proc. Natl. Acad. Sci. U.S.A.* **1989**, *86*, 9198–9202.

(17) Giovannangeli, C.; Montenay-Garestier, T.; Thuong, N. T.; Hélène, C. *Proc. Natl. Acad. Sci. U.S.A.* **1992**, *89*, 8631–8635.

(18) Cassidy, S. A.; Strekowski, L.; Wilson, W. D.; Fox, K. R. *Biochemistry* **1994**, *33*, 15338–15347.

(19) Nguyen, C. H.; Lhoste, J.-M.; Lavelle, F.; Bissery, M.-C.; Bisagni, E. *J. Med. Chem.* **1990**, *33*, 1519–1528.

(20) Nguyen, C. H.; Fan, E.; Riou, J.-F.; Bissery, M.-C.; Vrignaud, P.; Lavelle, F.; Bisagni, E. *Anti-Cancer Drug Des.* **1995**, *10*, 277–297.

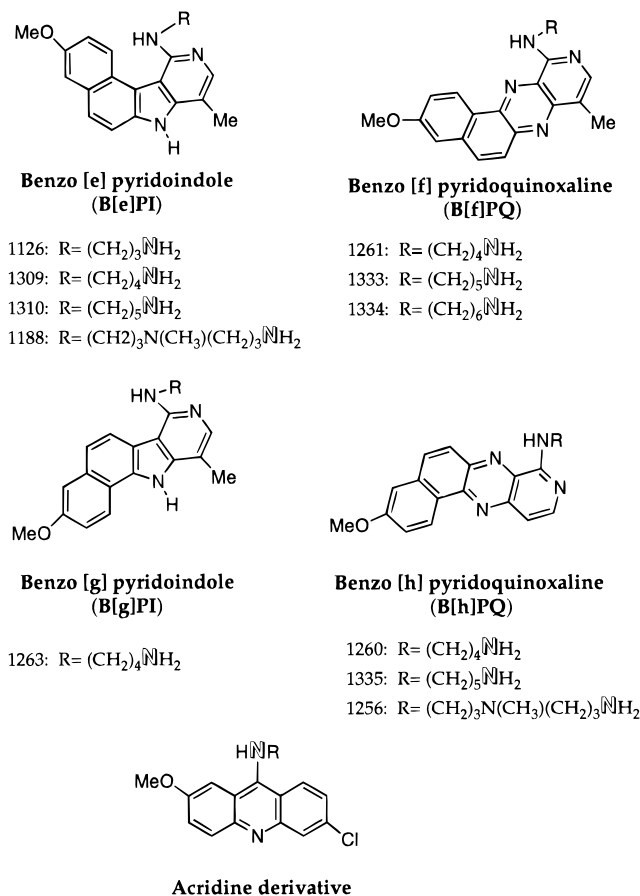


**Figure 1.** BPI (B[e]PI, B[g]PI), BPQ (B[f]PQ, B[h]PQ), and acridine derivatives. Oligonucleotides were attached to the terminal nitrogens on each of the hydrocarbon chains of the BPI and BPQ derivatives and to the nitrogen at position 9 of the acridine (specified nitrogens are outlined).

stabilize pyrimidine motif DNA triple helices in solution,<sup>21,22</sup> and can intercalate into both duplexes and triplexes but bind preferentially to triplexes.<sup>21–24</sup> In this study we have covalently linked BPIs and BPQs to the 5' end as well as to the interior (at an internucleotide phosphodiester linkage) of a 14-mer oligonucleotide (Figure 2). Triple helices formed with these modified oligonucleotides show remarkable improvement in stability under near physiological conditions as compared with both their unmodified and acridine-modified counterparts.

## Experimental Section

**Oligonucleotides.** Unmodified and acridine-modified (using 2-methoxy-6-chloro-9-aminoacridine) oligonucleotides were purchased from Eurogentec (Seraing, Belgium) or Genosys (Cambridge, England). The 14C3 oligonucleotide (Figure 2) contained a phosphorylated 5' end. The BPI- and BPQ-modified oligonucleotides were synthesized as described below. The linkage structure of the BPI-, BPQ-, and acridine-modified oligonucleotides is shown in Figure 3 for both the 5' end and internal modifications. The concentration of unmodified oligonucleotides was calculated using molar extinction coefficients at 260 nm

(21) Mergny, J. L.; Duval-Valentin, G.; Nguyen, C. H.; Perrouault, L.; Faucon, B.; Rougee, M.; Montenay-Garestier, T.; Bisagni, E.; Helene, C. *Science* **1992**, *256*, 1681–1684.

(22) Escudé, C.; Nguyen, C. H.; Mergny, J.-L.; Sun, J.-S.; Bisagni, E.; Garestier, T.; Hélène, C. *J. Am. Chem. Soc.* **1995**, *117*, 10212–10219.

(23) Pilch, D. S.; Waring, M. J.; Sun, J.-S.; Rougée, M.; Nguyen, C.-H.; Bisagni, E.; Garestier, T.; Hélène, C. *J. Mol. Biol.* **1993**, *232*, 926–946.

(24) Pilch, D. S.; Martin, M.-T.; Nguyen, C. H.; Sun, J.-S.; Bisagni, E.; Garestier, T.; Hélène, C. *J. Am. Chem. Soc.* **1993**, *115*, 9942–9951.

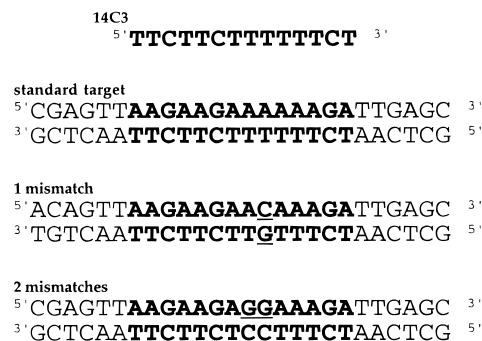


**Figure 2.** Sequence of unmodified and target oligonucleotides.

**Attachment through 5' end:**                      **Attachment through inter-nucleotide linkage:**

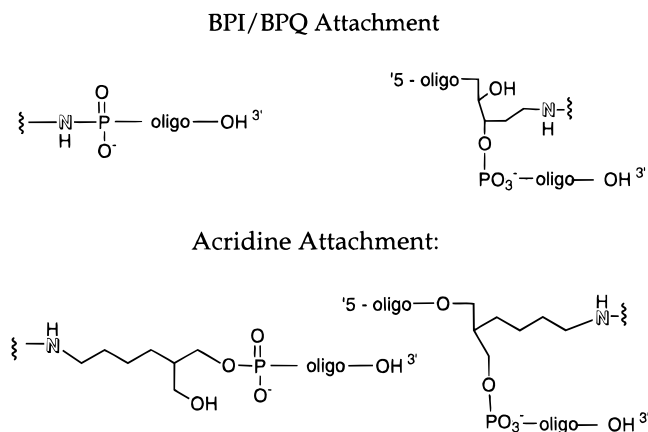


**Figure 3.** Linkage structure of BPIs, BPQs, and acridine to oligonucleotides. Outlined characters indicate the position of attachment to the intercalator. Note that, for BPI and BPQ derivatives, the NH group is that of the substituent R indicated in Figure 1, while for the acridine derivative the NH group is found at position 9 of the aromatic ring.

derived using a nearest-neighbor model.<sup>25,26</sup> The acridine-modified oligonucleotide concentration was calculated using  $\epsilon_{424} = 8845 \text{ M}^{-1}\cdot\text{cm}^{-1}$ .<sup>27</sup> The extinction coefficients for the BPI and BPQ conjugates were approximated by adding the experimentally derived extinction coefficient at 260 nm of the unconjugated BPIs or BPQs in H<sub>2</sub>O to the extinction coefficient for oligonucleotide 14C3 ( $\epsilon_{260} = 111\,300 \text{ M}^{-1}\cdot\text{cm}^{-1}$ ). All concentrations are given on a per strand basis.

**Syntheses.** To covalently link the BPQ and BPI derivatives to the 5' end of the oligomers,<sup>28,29</sup> 150  $\mu\text{g}$  of 5'-phosphorylated oligonucleotide 14C3 (Figure 2) was first precipitated as the hexadecyltrimethylammonium salt. The oligonucleotide salt was dissolved in 50  $\mu\text{L}$  of dry DMSO. A 5  $\mu\text{L}$  sample of *N*-methylimidazole and 25  $\mu\text{L}$  each of dipyridyl disulfide and triphenylphosphine solutions (1.2 M in DMSO) were added. After a 15 min incubation at room temperature, 5  $\mu\text{L}$  of triethylamine was added followed by the BPQ or BPI solution (20  $\mu\text{L}$ , 30 mM in DMSO). After 20 min the oligonucleotide was precipitated with LiClO<sub>4</sub> and purified by reversed phase HPLC using a linear acetonitrile gradient (0–40% CH<sub>3</sub>CN in 0.2 M ammonium acetate).

(25) Cantor, C. R.; Warshaw, M. M. *Biopolymers* **1970**, *9*, 1059–1077.

(26) Rougée, M.; Faucon, B.; Mergny, J. L.; Barcelo, F.; Giovannangeli, C.; Garestier, T.; Hélène, C. *Biochemistry* **1992**, *31*, 9269–9278.

(27) Asseline, U.; Delarue, M.; Lancelot, G.; Toulmé, J.-J.; Thuong, N. T.; Montenay-Garestier, T.; Hélène, C. *Proc. Natl. Acad. Sci. U.S.A.* **1984**, *81*, 3297–3301.

(28) Godovikova, T. S.; Zarytova, V. F.; Khalimskaya, L. M. *Bioorg. Khimiya* **1986**, *12*, 475–481.

(29) Mergny, J. L.; Boutorine, A. S.; Garestier, T.; Belloc, F.; Rougée, M.; Bulychev, N. V.; Koshkin, A. A.; Bourson, J.; Lebedev, A. V.; Valeur, B.; Thuong, N. T.; Hélène, C. *Nucleic Acids Res.* **1994**, *22*, 920–928.

Average yield 11%. The oligonucleotide–intercalator conjugates were characterized by UV–vis spectroscopy.

To attach the BPQ and BPI derivatives to the interior of the oligonucleotide,<sup>30</sup> first 100  $\mu\text{g}$  of oligo-15C3 (Figure 2) was dephurinated in a 100  $\mu\text{L}$  solution of 30 mM HCl and 1 mM EDTA for 22 h at 37  $^{\circ}\text{C}$ .<sup>31</sup> Following EtOH precipitation, the oligonucleotide was reacted with the BPQ or BPI derivative (2.5 mM), NaOAc, pH 5.2 (200 mM), and  $\text{NaBH}_3\text{CN}$  (50 mM) in a total volume of 100  $\mu\text{L}$  for 2 h. After ethanol precipitation, the oligonucleotide was recovered by reversed phase HPLC using a linear acetonitrile gradient (0–40%  $\text{CH}_3\text{CN}$  in 0.2 M ammonium acetate). Average yield 13%. The oligonucleotide–intercalator conjugates were characterized by UV–vis spectroscopy.

**Thermal Denaturation Studies.** Absorbance versus temperature curves were obtained using a Uvikon 940 spectrophotometer interfaced to an IBM computer. The temperature of the two six-cell holders was regulated by a Haake P2 circulating  $\text{H}_2\text{O}$ –glycerol (4:1) bath. The temperature was varied at a rate of 6  $^{\circ}\text{C}/\text{h}$  by a Haake PG20 thermoprogrammer descending from 62  $^{\circ}\text{C}$  (equilibrated for 70 min) to 0  $^{\circ}\text{C}$  (maintained for 70 min) and returning to 62  $^{\circ}\text{C}$ . The absorbance at 260 and at 600 nm was recorded every 8.3 min. Corrections for spectrophotometric instability were made by subtracting the absorbance at 600 nm from that at 260 nm. Experiments were carried out in two buffer systems. Buffer A (spermine buffer) contained 140 mM KCl, 15 mM sodium cacodylate, 1.5 mM  $\text{MgCl}_2$ , and 0.8 mM spermine, pH 6.9. Buffer B (no spermine) contained 125 mM NaCl, 15 mM sodium cacodylate, and 1.5 mM  $\text{MgCl}_2$ , pH 6.9.

In both buffer systems, there is some hysteresis in the heating and cooling curves, due to slow kinetics of formation and dissociation.<sup>26</sup> The difference between the cooling and heating curves in buffer A varied between 0.5 and 2  $^{\circ}\text{C}$  at the  $T_m$  value depending on the identity of the third strand. In buffer B, this variation was 1–4  $^{\circ}\text{C}$ . The reported  $T_m$  values were approximated as the maxima in  $dA/dT$  versus  $T$  plots of the heating curves. Values reported are an average of 2–4 experiments.

**Thermodynamic Calculations.** Hysteresis was minimal for many of the melting curves. Free energy values were, therefore, estimated for several of the complexes from their melting curves using a two-state model which assumes that the species with incomplete base pairing are not significantly populated.<sup>26,32</sup> A linear absorbance-*vs*-temperature relationship was assumed for the calculation of  $A_D$  and  $A_T$ , the absorbance of the double- and triple-stranded species, respectively. Equilibrium constants at different temperatures were then calculated, and the plot of  $\ln K_{\text{eq}}$  vs  $T^{-1}$  was used to determine  $\Delta G^{\circ}(37^{\circ}\text{C})$  as previously described.<sup>26,33–36</sup> The heating and cooling curves were analyzed separately, and it was found that the differences between the two values were insignificant. For the modified third strands (7 and 16), these calculations were performed after the subtraction of the melting curve obtained from a solution containing only the duplex target, in order to correctly fit the upper baseline. Errors are reported as the standard deviation.

**Molecular Modeling.** Molecular modeling by conformational energy minimization was carried out using the JUMNA program package.<sup>37</sup> The current version of JUMNA (version 7.2) allows for the inclusion of any number of modified nucleotides and tethered ligands into the calculation *via* the Nchem utility program, which is part of the JUMNA program package. B[e]PI derivatives attached through an internucleotide linkage were built using the InsightII graphical program (Biosym), and then charged and analyzed using Nchem to prepare the file containing geometrical parameters, atomic

charges, and flexibility information required by JUMNA. Nchem utilizes a Huckel–Del Re procedure for the calculation of the partial atomic charges.<sup>38</sup> Neither water nor positively charged counterions were explicitly included in the energy minimization. However, their effects were simulated by a sigmoidal, distance-dependent, dielectric function<sup>39</sup> and by assignment of half a negative charge to each phosphate group.

For reasons of computational cost, the triplexes studied were composed of 10 T·A·T base triplets to which the B[e]PI derivatives were introduced at the central position using the same linkage structure as the synthesized oligonucleotides (Figure 3). The coordinates of such a triple helix were derived from the previously published B-like triple helix<sup>40</sup> which is supported by NMR and vibrational spectroscopic data.<sup>40–45</sup> At the central part of the triplex, the *rise* parameter was doubled and the *twist* parameter was subsequently reduced in order to create an intercalation site. The interactive docking of the B[e]PI–triple helix complex was achieved manually by using InsightII to avoid strong steric clashes. In the early stages of energy minimization, the helicoidal variables were partially locked. Minimization was performed by successively decreasing the number of constraints until all variables were free to evolve and the energy convergence criterion was reached. We have previously checked that the results obtained are not affected by the order under which the constraints are released. To ensure that the energy-minimized triplexes were stable, several different docking structures were used. Computations were carried out on a Silicon Graphics 4D/420GTXB dual processor workstation, and the triplexes were visualized with the help of InsightII fully interfaced with JUMNA.

## Results and Discussion

**Syntheses.** The BPI- and BPQ-modified oligonucleotides used were synthesized as described in the Experimental Section. The third strand (Hoogsteen strand) in the triplex system contains only thymines and cytosines. To attach the intercalators to the phosphodiester backbone, we placed a purine at the position at which the intercalator was to be attached (oligonucleotide 15C3 in Figure 2). Purines hydrolyze more rapidly in acidic conditions than do pyrimidines,<sup>46,47</sup> leaving an aldehyde moiety for attachment of the intercalator through reductive amination to the backbone, and maintaining the three-carbon internucleotide distance between the phosphates.<sup>30</sup> The internally-modified acridine derivatives also maintain this distance (Figure 3).

The 15C3 oligonucleotide (Figure 2) was used for the depurination reaction-based synthesis. The intercalator–oligonucleotide product contains a “spacer” group at the position of attachment. Another possibility would have been to *replace* a pyrimidine base with a purine (the starting oligonucleotide would have therefore been a 14-mer rather than a 15-mer). However, molecular modeling experiments conducted in our laboratory had indicated that, upon intercalation into the triplex, the intercalator attached to the third strand spreads the duplex apart at the site of intercalation. Some experimental results,

(38) Lavery, R.; Zakrzewska, K.; Pullman, B. *J. Comput. Chem.* **1984**, *5*, 363–373.

(39) Lavery, R.; Sklenar, H.; Zakrzewska, K.; Pullman, B. *J. Biomol. Struct. Dyn.* **1986**, *3*, 989–1014.

(40) Ouali, M.; Letellier, R.; Adnet, F.; Liquier, J.; Sun, J.-S.; Lavery, R.; Taillandier, E. *Biochemistry* **1993**, *32*, 2098–103.

(41) Macaya, R. F.; Schultze, P.; Feigon, J. *J. Am. Chem. Soc.* **1992**, *114*, 781–783.

(42) Macaya, R. F.; Wang, E.; Schultze, P.; Sklenar, V.; Feigon, J. *J. Mol. Biol.* **1992**, *225*, 755–773.

(43) Radhakrishnan, I.; Patel, D. J.; Veal, J. M.; Gao, X. L. *J. Am. Chem. Soc.* **1992**, *114*, 6913–6915.

(44) Radhakrishnan, I.; Patel, D. J. *Structure* **1993**, *1*, 135–152.

(45) Radhakrishnan, I.; Patel, D. J. *Structure* **1994**, *2*, 17–32.

(46) Kotchetov, N. K.; Budovskii, E. J. *Organic Chemistry of Nucleic Acids*; Plenum Press: New York, 1972; Part B, pp 425–443.

(47) Zielonacka-Lis, E. *Nucleosides Nucleotides* **1989**, *8*, 383–405.

(30) Vasseur, J.-J.; Peoc'h, D.; Rayner, B.; Imbach, J.-L. *Nucleosides Nucleotides* **1991**, *10*, 107–117.

(31) Bailly, V.; Verly, W. G. *Biochem. J.* **1987**, *242*, 565–572.

(32) Cantor, C.; Schimmel, P. *Biophysical Chemistry*; W. H. Freeman and Co.: San Francisco, 1980; Vol. 3, pp Chapter 22.

(33) Breslauer, K.; Sturtevant, J.; Tinoco, I. J. *J. Mol. Biol.* **1975**, *99*, 549–65.

(34) Albergo, D.; Marky, L.; Breslauer, K.; Turner, D. *Biochemistry* **1981**, *20*, 1409–13.

(35) Petersheim, M.; Turner, D. H. *Biochemistry* **1983**, *22*, 256–263.

(36) Wang, S.; Kool, E. T. *Biochemistry* **1995**, *34*, 4125–4132.

(37) Lavery, R. In *Structure and Expression*; Olson, W. K., Sarma, R. H., Sarma, M. H., Sundaralingham, M., Eds.; Adenine Press: New York, 1988; Vol. 3, pp 191–211.

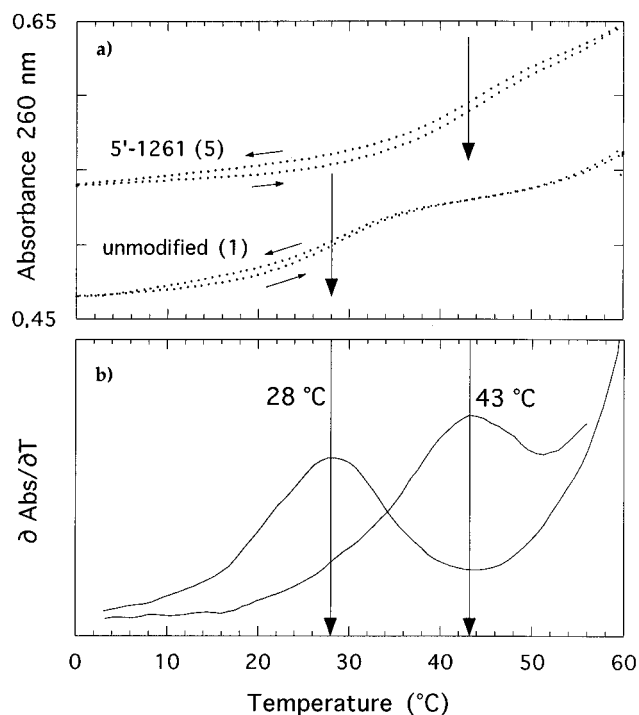


**Figure 4.** (a) Example of heating and cooling curves. The figure shows the corrected absorbance at 260 nm for the duplex target (1  $\mu\text{M}$ ) in buffer A in the presence of (i) 1.5  $\mu\text{M}$  unmodified third strand (1) or (ii) 1.5  $\mu\text{M}$  oligonucleotide 6 (Table 1). Arrows indicate the heating and cooling curves. (b) First derivative of the heating curves in (a).

published<sup>48</sup> as well as unpublished, have also shown that the “addition” rather than the “replacement” of a base resulted in the more favorable alignment of the third strand with the duplex.

**Thermal Denaturation Studies.** Hyperchromicity at 260 nm accompanies the dissociation of the third strand from the duplex. The midpoint of this transition ( $T_m$ ) gives a relative measure of stability of the triple helix. To study the ability of these new conjugates to stabilize triple helices, UV thermal melting studies were performed with each conjugate in the presence of a 26 base pair target duplex (Figure 2). A typical melting curve profile is shown in Figure 4. Comparisons were made with the naked third strand (14C3) and with the nondepurinated oligonucleotide, 15C3, as well as with the acridine conjugates. The results of these studies are shown in Table 1.

As even small changes in ionic concentrations can have significant effects,<sup>26,49</sup> two somewhat different buffers were chosen to determine if the same trends in stability would be seen. The main difference between these two buffers, in terms of triple helix stability, is the presence of spermine in buffer A. Spermine is present in physiological conditions;<sup>50–52</sup> however, much of it may be bound to other biomolecules, rendering the free concentration uncertain. All the  $T_m$  values obtained in buffer A were higher than their counterparts obtained in buffer B, as is to be expected, since spermine has been shown to significantly stabilize the formation of triple helices.<sup>49</sup> However, in comparing general trends, the *relative* stabilities of the triplexes formed with the various conjugates and the  $\Delta T_m$  values were similar.

(48) Zhou, B. W.; Puga, E.; Sun, J. S.; Garestier, T.; Hélène, C. *J. Am. Chem. Soc.* **1995**, *117*, 10425–10428.

(49) Singleton, S. F.; Dervan, P. B. *Biochemistry* **1993**, *32*, 13171–13179.

(50) Tabor, C.; Tabor, H. *Annu. Rev. Biochem.* **1976**, *45*, 285–306.

(51) Sarhan, S.; Seiler, N. *Biol. Chem. Hoppe-Seyler* **1989**, *370*, 1279–1284.

(52) Alberts, B.; Bray, D.; Lewis, J.; Raff, M.; Roberts, K.; Watson, J. D. *Molecular Biology of the Cell*, 2nd ed.; Garland Publishing, Inc.: New York, 1983; p 286.

All of the conjugates formed stronger triple helices than did the unmodified third strand (14C3). The most dramatic stabilization was seen with oligonucleotides 7 (a B[h]PQ attached to the 5' end) and 13 (a B[e]PI attached to the interior). In the presence of spermine (buffer A), these oligonucleotides have  $T_m$  values of 51 and 54 °C, respectively, which is an increase of 23 and 26 °C compared with the unsubstituted third strand and an increase of 6 and 19 °C versus their acridine counterparts. In buffer B, they have  $T_m$  values of 38 °C and 37 °C ( $\Delta T_m$  values of 27 and 26 °C versus the unmodified third strand and 13 °C and 14 °C versus their acridine counterparts). The two other 5'-modified B[h]PQ derivatives, oligonucleotides 8 and 9, also showed a substantial stabilization. The other 5'-modified oligonucleotides also showed stabilization, though not better than that seen with the 5'-acridine-modified oligonucleotide 10. Oligonucleotides with intercalators attached to the interior showing significant stabilization aside from 13 include 11, 12, and 14 (B[e]PIs attached) and 16 (B[f]PQ). The B[h]PQ and B[g]PI conjugates at this position gave no notable enhancement in binding affinity over the acridine derivative 21. As is to be expected, the nondepurinated oligonucleotide 15C3 showed little or no formation of triplex.

That oligonucleotide 13 shows the greatest stabilization of all the oligonucleotides tested is noteworthy. This is the first example of an intercalator attached to an internal position of a probe oligonucleotide showing significant stabilization of a triple helix, and, in fact, showing greater stabilization than the corresponding 5' oligonucleotide conjugate.

The values of  $\Delta G^\circ$  at 37 °C were estimated from the melting curves for the oligonucleotide without an intercalator (1) and for the oligonucleotide covalently attached to B[h]PQ 1260 (5' end) or to B[f]PQ 1261 (internal attachment) (7 and 16). The  $\Delta G^\circ$  (37 °C) values were  $-6.3 \pm 0.3$ ,  $-10.0 \pm 0.1$ , and  $-9.2 \pm 0.1$  kcal·mol<sup>-1</sup>, respectively. These results indicate that attachment of an intercalating agent to either an interior site or the 5' end stabilizes the complexes by 3–4 kcal·mol<sup>-1</sup> at 37 °C.

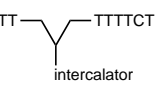
Which intercalator is the best at stabilizing the triple helix? Comparing the four types of intercalators linked at the internal position having a  $-(\text{CH}_2)_4-$  linker arm, the trend in order of stability is B[f]PQ  $\geq$  B[e]PI  $>$  B[h]PQ  $>$  B[g]PI. With a linker arm of  $-(\text{CH}_2)_3\text{NMe}(\text{CH}_2)_3-$ , B[e]PI is better than B[h]PQ. Interestingly, the same B[h]PQ intercalator, when attached to the 5' end by a  $-(\text{CH}_2)_4-$  linker arm, shows a dramatic increase in terms of its relative stability, namely: B[h]PQ  $\gg$  B[f]PQ  $\geq$  B[e]PI  $\sim$  B[g]PI. Several factors may explain this reversal in stability: (i) the orientation of the intercalator with regards to the triplex may be different in both cases; (ii) the duplex–triplex junction is an important site of intercalation for the 5' end attachments; (iii) finally, the different linkage structures are likely to play an important role.

The effect of varying arm lengths on the stability of the triplexes can be examined for several of the derivatives. The results at the internal position for the B[e]PI derivatives indicate that the chain length can have a considerable effect:  $-(\text{CH}_2)_5-$   $\gg$   $-(\text{CH}_2)_3-$   $\cong$   $-(\text{CH}_2)_4-$ . Comparisons among internally attached B[f]PQ and 5' attached B[h]PQ derivatives do not show as dramatic a difference, though the effect of chain length is nevertheless significant. These differences in stabilization demonstrate the importance of chain length and the charge of the chain on the binding affinity of triplex-forming oligonucleotides for their target.<sup>53,54</sup> Energy minimization with a molec-

(53) Chen, J.-k.; Weith, H. L.; Grewal, R. S.; Wang, G.; Cushman, M. *Bioconjugate Chem.* **1995**, *6*, 473–482.

(54) Orson, F. M.; Kinsey, B. M.; McShan, W. M. *Nucleic Acids Res.* **1994**, *22*, 479–484.

**Table 1.** Thermal Melting Data of Triplex to Duplex Transitions.

	ligand	linker arm	$T_m$ ( $\Delta T_m$ ) (°C)	
			buffer A	buffer B
<b>1</b>	oligonucleotide 14C3 (unmodified)		28	11
<b>2</b>	oligonucleotide 15C3		9	not detected
		5' End intercalator—TTCTTCTTTTCT		
<b>3</b>	B[e]PI 1126	—(CH <sub>2</sub> ) <sub>3</sub> —	35 (7)	19 (7)
<b>4</b>	B[e]PI 1309	—(CH <sub>2</sub> ) <sub>4</sub> —	41 (13)	not tested
<b>5</b>	B[g]PI 1263	—(CH <sub>2</sub> ) <sub>4</sub> —	41 (13)	not tested
<b>6</b>	B[f]PQ 1261	—(CH <sub>2</sub> ) <sub>4</sub> —	43 (15)	23 (12)
<b>7</b>	B[h]PQ 1260	—(CH <sub>2</sub> ) <sub>4</sub> —	51 (23)	38 (27)
<b>8</b>	B[h]PQ 1335	—(CH <sub>2</sub> ) <sub>5</sub> —	47 (19)	not tested
<b>9</b>	B[h]PQ 1256	—CH <sub>2</sub> ) <sub>3</sub> NMe(CH <sub>2</sub> ) <sub>3</sub> —	49 (21)	26 (15)
<b>10</b>	acridine		45 (17)	25 (14)
		Internal Attachment TTCTTCTT—  —TTTTCT		
<b>11</b>	B[e]PI 1126	—(CH <sub>2</sub> ) <sub>3</sub> —	44 (16)	31 (20)
<b>12</b>	B[e]PI 1309	—(CH <sub>2</sub> ) <sub>4</sub> —	43 (15)	31 (20)
<b>13</b>	B[e]PI 1310	—(CH <sub>2</sub> ) <sub>5</sub> —	54 (26)	37 (26)
<b>14</b>	B[e]PI 1188	—(CH <sub>2</sub> ) <sub>3</sub> NMe(CH <sub>2</sub> ) <sub>3</sub> —	43 (15)	not tested
<b>15</b>	B[g]PI 1263	—(CH <sub>2</sub> ) <sub>4</sub> —	33 (5)	not tested
<b>16</b>	B[f]PQ 1261	—(CH <sub>2</sub> ) <sub>4</sub> —	45 (17)	30 (19)
<b>17</b>	B[f]PQ 1333	—(CH <sub>2</sub> ) <sub>5</sub> —	41 (13)	not tested
<b>18</b>	B[f]PQ 1334	—(CH <sub>2</sub> ) <sub>6</sub> —	40 (12)	not tested
<b>19</b>	B[h]PQ 1260	—(CH <sub>2</sub> ) <sub>4</sub> —	39 (11)	24 (13)
<b>20</b>	B[h]PQ 1256	—CH <sub>2</sub> ) <sub>3</sub> NMe(CH <sub>2</sub> ) <sub>3</sub> —	38 (10)	25 (14)
<b>21</b>	acridine		35 (7)	23 (12)

<sup>a</sup> 1  $\mu$ M duplex and 1.5  $\mu$ M third strand. Buffer A: 140 mM KCl, 15 mM sodium cacodylate, 1.5 mM MgCl<sub>2</sub>, 0.8 mM spermine, pH 6.9. Buffer B: 125 mM NaCl, 15 mM sodium cacodylate, 1.5 mM MgCl<sub>2</sub>, pH 6.9.

**Table 2.**  $T_m$  Values (°C) of Triplexes with Mismatches in the Target Duplex Sequence

probe strand	target duplex				
	no mismatch		1 mismatch		two mismatches
	buffer A	buffer B	buffer A	buffer B	buffer A
unmodified 14C3 ( <b>1</b> )	28	11	18	<8	not detected
5'-1260 ( <b>7</b> )	51	38	34	20	17
5'-1256 ( <b>9</b> )	49	26	34	not tested	not tested
interior-1256 ( <b>20</b> )	38	25	21	not tested	6
interior-acridine ( <b>21</b> )	35	23	29	not tested	8

ular modeling program confirmed the results observed with the internally attached B[e]PI derivatives. At the 5' position, we obtained better stabilization with —(CH<sub>2</sub>)<sub>4</sub>— than with —(CH<sub>2</sub>)<sub>3</sub>—. Results with other systems (unpublished results<sup>55</sup>) in which the effect of chain length at the 5' end was investigated indicated that the —(CH<sub>2</sub>)<sub>3</sub>— group is too short, whereas longer chain lengths (—(CH<sub>2</sub>)<sub>4</sub>— to —(CH<sub>2</sub>)<sub>6</sub>—) were approximately equivalent in allowing the intercalator to stabilize triple helix formation.

**Sequence Specificity.** In designing oligonucleotides which bind strongly to their target sequences, it is important not only to obtain strong binding but also to maintain selectivity. To study this aspect, two other duplex targets with one or two mismatches in the middle of the target sequence (Figure 2) were tested in the presence of **1**, **7**, **9**, **20**, and **21**. The  $T_m$  values obtained are shown in Table 2. The stabilization seen with the BPQ oligonucleotide—intercalator derivatives was greatly decreased in the case of only one mismatch in all three cases whether attached to the 5' end or internally. Both the acridine-modified and the unmodified third strands show less of a drop in stability. A second mismatch further decreased the stability of all the oligonucleotide—intercalator conjugates. This dem-

**Table 3.** Energy Contribution of B[e]PI-Triple Helical Complexes with Linker Arms of Various Lengths for Conformer II<sup>a</sup>

linker arm	$E_{TH}$	$E_{TH-B[e]PI}$	$E_{B[e]PI}$	$E_C$
—(CH <sub>2</sub> ) <sub>2</sub> —	-479	-77	99	-457
—(CH <sub>2</sub> ) <sub>3</sub> —	-477	-99	93	-483
—(CH <sub>2</sub> ) <sub>4</sub> —	-481	-86	75	-492
—(CH <sub>2</sub> ) <sub>5</sub> —	-492	-88	79	-501
—(CH <sub>2</sub> ) <sub>6</sub> —	-490	-86	91	-485

<sup>a</sup> The components of the complexation energy ( $E_C$ ), namely, the energy of the triple helix ( $E_{TH}$ ), of the B[e]PI residue ( $E_{B[e]PI}$ ), and of the interaction ( $E_{TH-B[e]PI}$ ), are shown. The units of energy are kilocalories per mole.

onstrates that recognition selectivity is maintained with the attachment of the BPQ intercalators to the 5' end or at an internal position of the oligonucleotide.

**Molecular Modeling.** Molecular modeling by conformational energy minimization was performed to predict the optimal length of the linker arm of the B[e]PI residue as an internally-incorporated triplex stabilizer. The results are given in Table 3 and Figure 5. There are two orientations of the intercalated B[e]PI molecule. The methoxy group is placed either near the pyrimidine strand of the Watson—Crick duplex (conformer I) or in the narrow groove formed between the purine strand of the Watson—Crick duplex and the third strand (conformer II).

(55) Silver, G. C.; Nguyen, C. H.; Boutorine, A. S.; Bisagni, E.; Garestier, T.; Héline, C. *Bioconjugate Chem.*, in press.

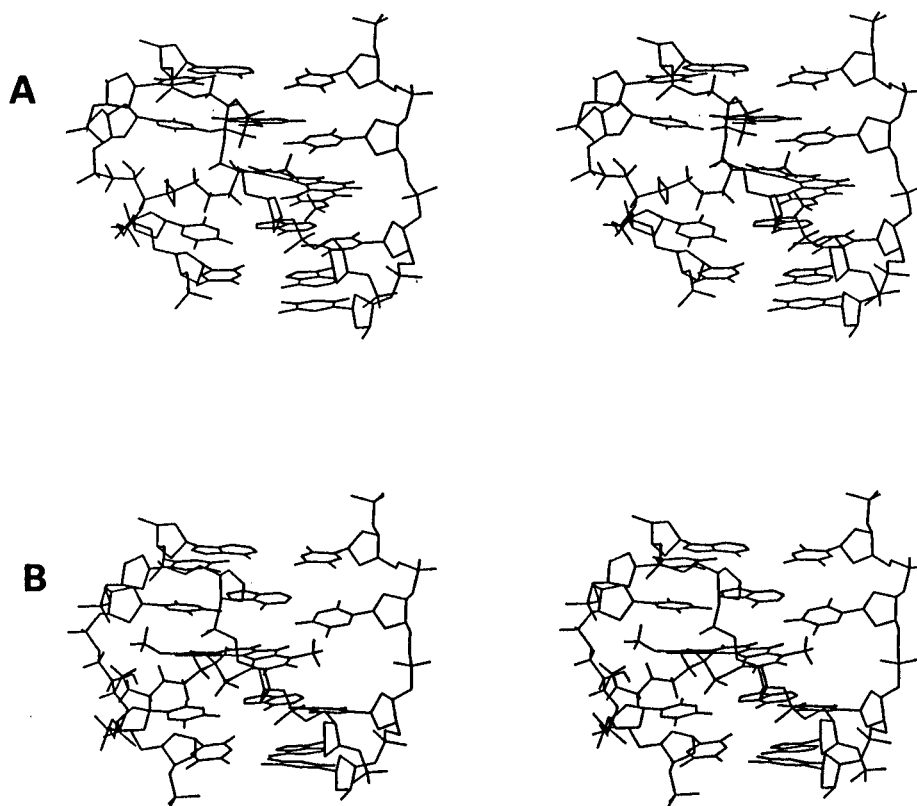


**Figure 5.** Stereoview of the triplex model with an internally incorporated B[e]PI derivative attached through the terminal amino group of the linker arm  $-(\text{CH}_2)_n-$  to an abasic site. The triplex is composed of T·A·T triplets around the intercalation site of B[e]PI. Two conformers of intercalated B[e]PI are possible. Conformer I is shown in (A) with  $n = 3$  (the most stable length for this conformer). However, conformer II (with the methoxy group pointing in the opposite direction) shows greater triplex stability and is shown in (B) with  $n = 5$ , the optimal length.

Conformer II requires a longer linker (at least a tetramethylenechain) as compared to conformer I in which a di- or trimethylene linker could be used.

Modeling shows that conformer II is energetically favored as compared to conformer I. It is worth noting that a previous study suggested that B[e]PI derivatives free in solution intercalate in a configuration similar to that of conformer II.<sup>2</sup> A pentamethylene linker arm gives the best complexation energy which principally comes from the conformational energy terms of the triple helix and B[e]PI residue since there is no significant difference between the interaction energy terms of the B[e]PI residue and the triple helix with a linker ranging from tetra- to hexamethylene. These molecular modeling studies are in agreement with the experimental results which show that a  $-(\text{CH}_2)_5-$  linker gives better stabilization than a shorter linker when B[e]PI is inserted within the oligonucleotide sequence.

### Conclusion

We have synthesized novel oligonucleotide conjugates which are shown to significantly stabilize pyrimidine motif triple helices. Triplex DNA is now formed in near physiological conditions and at 37 °C. Comparisons made with acridine conjugates in the same conditions show that these novel conjugates are significantly more stable. This is the first example of an oligonucleotide conjugate with the intercalator attached at an internal position showing an important stabilization of triple helical DNA.

**Acknowledgment.** We thank Jean-Louis Mergny for comments on the manuscript. G.C.S. acknowledges the Ministère des Affaires Etrangères du Gouvernement Français for a Chateaubriand Fellowship as well as the support of the National Science Foundation (Grant INT 9403368).

JA961304H